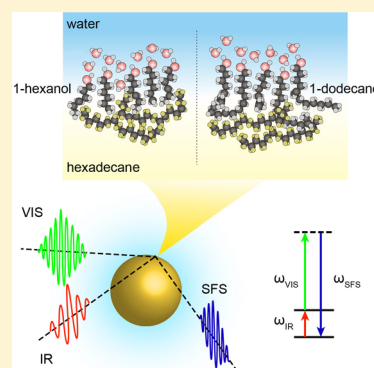


# From Hydrophobic to Hydrophilic: The Structure and Density of the Hexadecane Droplet/Alkanol/Water Interface

Yixing Chen,<sup>†</sup> Kailash C. Jena,<sup>†,‡</sup> and Sylvie Roke<sup>\*,†</sup><sup>†</sup>Laboratory for fundamental BioPhotonics (LBP), Institute of Bioengineering (IBI), School of Engineering (STI), École Polytechnique Fédérale de Lausanne (EPFL), CH-1015, Lausanne, Switzerland<sup>‡</sup>Department of Physics, Indian Institute of Technology Ropar, Rupnagar, 140001, India

## S Supporting Information

**ABSTRACT:** The molecular structure of the hexadecane droplet/alkanol/water interface has been investigated using vibrational sum frequency scattering and second harmonic scattering. This combination of methods allows us to investigate the interfacial alkyl chain conformation of the oil and several alkanols, ranging from 1-pentanol to 1-dodecanol, the orientational distribution of the methyl groups, the surface density of the alkanols, as well as the orientational alignment of water. For the hexadecane/1-dodecanol/water interface, dodecanol alkyl chains form a fluid layer with a wide distribution of tilt angles of the terminal CH<sub>3</sub> groups. Indistinguishable spectra are recorded for the alkanol alkyl chains of 1-pentanol, 1-hexanol, 1-octanol, and 1-dodecanol, and alkanols with chain length longer than 6 C atoms all form films with similar densities. In contrast, the alkyl chains of the oil phase are relatively more distorted with respect to the pure oil/water interface for alkanols with shorter chain lengths. The projected surface area of a saturated film of hexanol is  $29 \pm 5 \text{ \AA}^2$ , which requires a free energy of adsorption of  $\Delta G = -26.3 \pm 0.7 \text{ kJ/mol}$ . In addition, with increasing alkanol density the interfacial water structure loses its initial orientational alignment, which matches with the added number of interfacial 1-hexanol molecules. The found structures differ significantly from those reported on the alkanol/water and alkanol/air interface and charged surfactant/oil/water interface.



## INTRODUCTION

The structural elements that form the building blocks of life are composed of aqueous regions that are in contact with hydrophobic domains or cores, such as the structures found in membranes, peptides, and proteins. The transition from a hydrophilic to a hydrophobic environment is therefore essential for understanding fundamental aspects of living systems. The quantitative study of this type of structures and the related interactions started over a century ago, when interfacial tension studies were performed on insoluble monolayers.<sup>1–3</sup> It was suggested that molecules are surface active when they lower the energy of the interface. This lowering of the interfacial energy was explained in terms of solubility: When a molecule has parts that dissolve better in a polar/nonpolar solvent it will orient itself in a configuration of lowest energy, that is, partially dissolved in oil and partially dissolved in water. Alkanols are uncharged amphiphilic molecules with a hydrophobic part that dissolves well in an oil phase and a hydrophilic part that dissolves well in a water phase and they form essential building blocks that provide a transition between hydrophobic and hydrophilic environments. Depending on the chain length, the partitioning between water and oil changes, as well as the free energy of transfer from the oil to the water phase. Figure 1 shows the partitioning coefficient derived from the Ostwald solubility (A) and the free energy of transfer (B) for several 1-alkanols in the hexadecane/water system, which is exemplary of a true hydrophobic liquid in contact with water (used, for

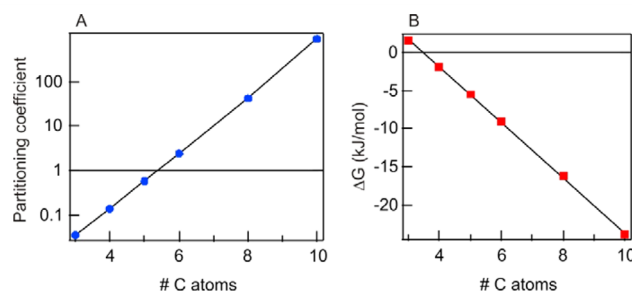


**Figure 1.** Thermodynamic data of solute transfer. (A) Partitioning coefficient of several 1-alkanols with chain lengths from C3–C10, derived by dividing the Ostwald solubilities of the respective 1-alkanol in hexadecane by that of water. (B) Free energies of transfer from water to hexadecane. The data was adapted from ref 4.

example, to estimate the activity of pharmaceuticals<sup>4</sup>). It can be seen that 1-propanol, 1-butanol, and 1-pentanol are more soluble in water than in oil, while for 1-hexanol, 1-heptanol, 1-octanol, and 1-decanol the reverse applies. The free energy of transfer from water to hexadecane shows a similar trend, but here only 1-propanol has a positive free energy of transfer to the oil phase. How the transition from oil to water occurs on

Received: May 22, 2015

Revised: July 1, 2015

Published: July 7, 2015

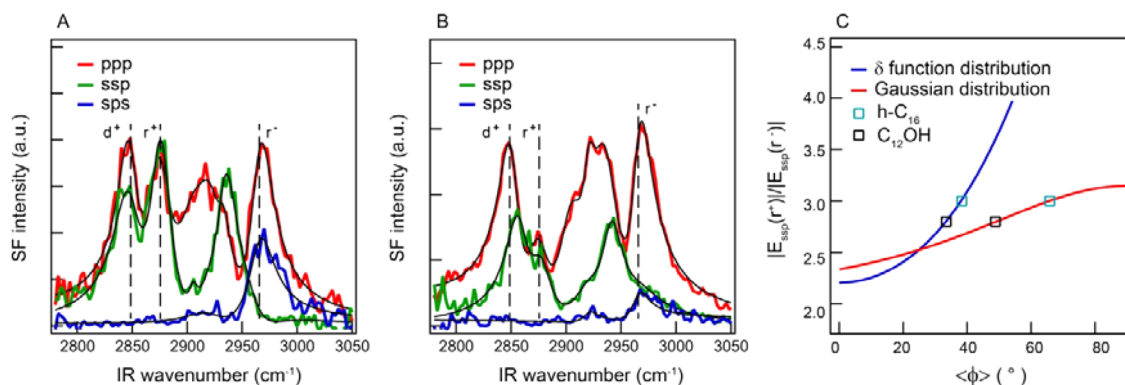


**Figure 2.** The surface structure of 1-dodecanol and hexadecane at the hexadecane nanodroplet/water interface. (A,B) SFS spectra of the C–H stretch modes of the 1-dodecanol/d<sub>34</sub>-hexadecane droplet interface (A) and the d<sub>25</sub>-1-dodecanol/hexadecane droplet interface (B) in D<sub>2</sub>O. The spectra are recorded in three different polarization combinations, PPP (red), SSP (green), and SPS (blue). The black lines are fits to the spectra. (C) Calculated r<sup>+</sup>/r<sup>-</sup> amplitude ratio as a function of the average tilt angle  $\phi$  of the end methyl group of the alkyl chain with respect to the surface normal. The distribution of tilt angles is represented by both a  $\delta$ -function and a Gaussian function (assuming an angular full width at half-maximum of 70°). For the hyperpolarizability ratio  $\beta_{aac}/\beta_{ccc}$  we have used the value 3.4.<sup>40</sup> The average radius  $R$  of the nanodroplets is 115 nm (1 vol %). For the opening ( $\beta$ ) and scattering ( $\theta$ ) angle, we used  $\beta = 5^\circ$  and  $\theta = 35^\circ$  (which represent the values inside the cuvette), and appropriate refractive index values are given in Supporting Information Table S2.

the molecular level, whether this transition requires a particular structure of the alkanol, the water or the oil, and whether it depends critically on chain length is not conveyed by the data in Figure 1.

Molecular level information about the electronic order present in the interfacial layer can be obtained from X-ray reflection measurements in combination with appropriate modeling of ordered monolayers of alkanols on water (see, for example, refs 5 and 6). Molecular level insight combined with intrinsic interfacial sensitivity can also be obtained by means of sum frequency generation (SFG), a vibrational coherent interface spectroscopy that measures the combined infrared (IR) and Raman spectrum of molecules in non-centrosymmetric environments such as interfaces.<sup>7–9</sup> The majority of the vibrational SFG studies have been performed on the air/alkanol interface with a focus on the alkyl chain conformation,<sup>10,11</sup> the water/alkanol/air interface,<sup>12–16</sup> with a focus on both the alkyl chain conformation and the effects of hydration.<sup>15,16</sup> The choice for these systems is likely determined by the experimental geometry, which permits unhindered access to the interface. Studies of the liquid/liquid oil/water interface are more challenging for several reasons: the optical beams need to pass through one of the often absorptive phases,<sup>17</sup> the formation of a planar oil/water interface is nontrivial, and it often consists of a heterogeneous structure<sup>18</sup> made up of nano- and microscopic islands, which are critically influenced by the tiniest amount of intrinsic impurities that might be present.<sup>19</sup> Therefore, the focus is often on one aspect, namely the water structure<sup>20–23</sup> or the alkyl chain conformation.<sup>17</sup> The latter can be probed by measuring SFG spectra in the C–H stretch region. The amplitude ratio (referred to as d<sup>+</sup>/r<sup>+</sup> ratio) of the symmetric methylene (d<sup>+</sup> at ~2850 cm<sup>-1</sup>) and the symmetric methyl (r<sup>+</sup> at ~2876 cm<sup>-1</sup>) stretch vibrational modes is a common empirical indicator for the conformation of alkyl chains.<sup>24–26</sup> A value of d<sup>+</sup>/r<sup>+</sup>  $\ll$  1 is associated with a stretched all-trans chain conformation, whereas a value of d<sup>+</sup>/r<sup>+</sup>  $>$  1 indicates that gauche defects dominate the measured SFG spectrum. Using selective deuteration it is possible to independently probe the surfactant and the oil molecules, since C–D and C–H modes vibrate at different frequencies.<sup>26</sup>

In order to obtain full molecular level insight into the molecular structural aspects of the transition from a hydrophobic to an aqueous phase without being hindered by the above restrictions, we use a dispersion of ~100 nm (radius) hexadecane droplets in water that also contains 1-pentanol, 1-hexanol, 1-octanol, or 1-dodecanol. We study the transition from the hydrophobic to aqueous phase and the role played by hydrophobic interactions by determining the alkyl chain conformation of the alkanols and the oil, the surface density of the alkanols, and the structural changes imposed on the water using a combination of second harmonic<sup>27–29</sup> (SH) and sum frequency scattering<sup>29,30</sup> (SFS). Second harmonic<sup>31</sup> scattering<sup>27,32–34</sup> (SHS) is a process that occurs only in noncentrosymmetric materials. The SHS signal can be used as a probe for the interfacial water around nanoscopic droplets and reports on the difference in dynamic orientational directionality of the water molecules in the interfacial region compared to the orientational directionality in the bulk solution.<sup>31,35–37</sup> On the other hand, the SFS signal can be used to probe the chemical composition, alkyl chain conformation, and density of the droplet/water interface.<sup>29,38,39</sup> Using selective deuteration and probing the C–H stretch mode region we have measured the conformation of the alkyl chains present on the 1-pentanol, 1-hexanol, 1-octanol, and 1-dodecanol/d<sub>34</sub>-hexadecane interface and the d<sub>11</sub>-1-pentanol, d<sub>13</sub>-1-hexanol, d<sub>17</sub>-1-octanol, and d<sub>25</sub>-1-dodecanol/hexadecane interface. Starting with the hexadecane/1-dodecanol/water interface, we find that the relative chain conformation represents that of a fluid layer with a wide distribution of tilt angles of the terminal CH<sub>3</sub> groups. Changing the chain lengths of the alkanol, the alkanol alkyl chains adopt a conformation that generates indistinguishable SF spectra. Comparing the amplitude of the spectra it appears that the alkanols with chain lengths longer than 6 C atoms all form films with comparable chain densities. In contrast, the alkyl chains of the oil phase are relatively more distorted with respect to the pure oil/water interface for shorter alkanol alkyl chains. For 1-hexanol, we measured the surface density more accurately by means of an SFS isotherm, finding a projected surface density of  $29 \pm 5 \text{ \AA}^2$  and a free energy of adsorption of  $\Delta G = -26.3 \pm 0.7 \text{ kJ/mol}$ . SHS measurements on the same system show that with increasing 1-hexanol density the interfacial water structure

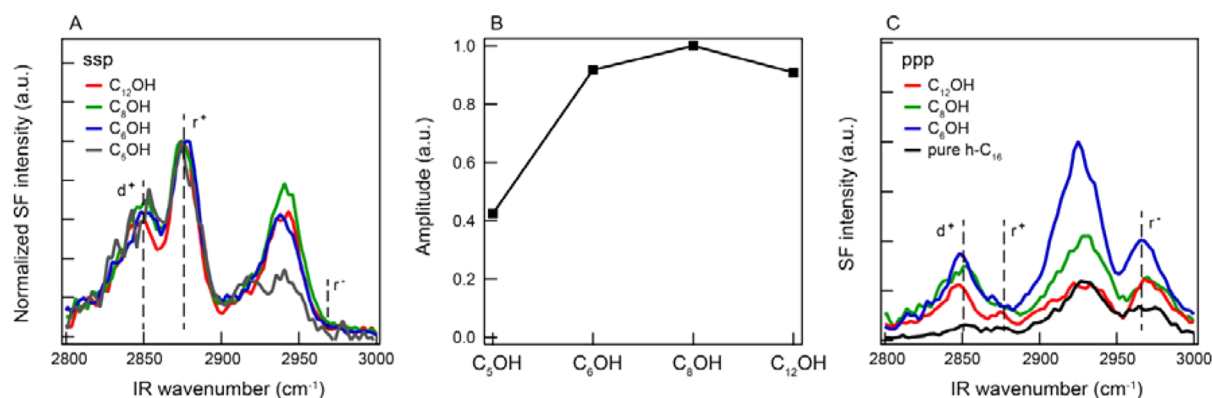


**Figure 3.** (A) Normalized spectra in SSP polarization for 1-pentanol, 1-hexanol, 1-octanol, and 1-dodecanol at the interface of d<sub>34</sub>-hexadecane droplets in water (see the Materials and Methods for details on droplet size and concentrations). The spectra were normalized to the s-CH<sub>3</sub> stretch mode. (B) Spectral amplitude corresponding to the data in panel A. (C) Hexadecane spectra for the same concentration but now with deuterated alkanol recorded in PPP polarization.

loses its initial orientational alignment in a way that matches with the added number of interfacial 1-hexanol molecules. The found conformations differ significantly from that reported at the alkanol/water and alkanol/air interface.

In what follows we will first present and analyze SFS spectra of the 1-dodecanol/hexadecane/water interface. Then we will change the chain length and investigate the isotherm of 1-hexanol. Finally we will turn to the water structure and discuss our findings in a broader scope.

## RESULTS AND DISCUSSION

**The Surface Structure of 1-Dodecanol.** Figure 2 shows SFS spectra of the C–H stretch modes of the 1-dodecanol/d<sub>34</sub>-hexadecane droplet interface (A) and the d<sub>25</sub>-1-dodecanol/hexadecane droplet interface (B) in D<sub>2</sub>O. The spectra are recorded in three different polarization combinations: SSP, PPP, and SPS. Here the three letter code represents the polarization of each beam from high frequency to low frequency, with P(S) referring to light polarized parallel (perpendicular) to the scattering plane. The spectra are fitted according to the procedure described in the Supporting Information. Figure 2C shows a calculation of the amplitude ratio of the symmetric methyl (r<sup>+</sup>, at ~2876 cm<sup>-1</sup>) and the antisymmetric methyl (r<sup>-</sup>, at ~2965 cm<sup>-1</sup>) stretch modes. This ratio is used to derive the average tilt angle ⟨ϕ⟩ of the methyl group of the alkyl chains of the 1-dodecanol and hexadecane with respect to the surface normal.

Starting with the SSP spectrum of 1-dodecanol and hexadecane (green lines in Figure 2A,B), it can be seen that the following peaks are present:<sup>11</sup> the symmetric (s) CH<sub>2</sub> stretch mode (~2850 cm<sup>-1</sup>, d<sup>+</sup>), the s-CH<sub>3</sub> stretch mode (~2876 cm<sup>-1</sup>, r<sup>+</sup>), the antisymmetric (as) CH<sub>3</sub> stretch mode (~2965 cm<sup>-1</sup>, r<sup>-</sup>), the s-CH<sub>2</sub>–Fermi resonance (~2905 cm<sup>-1</sup>, d<sup>+</sup><sub>FR</sub>), the s-CH<sub>3</sub>–Fermi resonance (~2933 cm<sup>-1</sup>, r<sup>+</sup><sub>FR</sub>), and the as-CH<sub>2</sub> stretch mode (~2920 cm<sup>-1</sup>, d<sup>-</sup>). The latter three modes are broad and overlap.<sup>16,41</sup> Fitted values can be found in Supporting Information Table S1. The obtained d<sup>+</sup>/r<sup>+</sup> amplitude ratio for 1-dodecanol is 0.7 ± 0.2, while that for hexadecane is 1.1 ± 0.2. This shows that there are fewer visible gauche defects in the spectra of the alkyl chains of the 1-dodecanol than in the alkyl chains of the hexadecane.

Comparing the three polarization combinations, we observe that the spectra are different. Specifically, it can be seen that the SSP spectra in Figure 2A,B show less antisymmetric character

and have a smaller relative d<sup>+</sup>/r<sup>+</sup> ratio than the PPP spectra. The relative phase of the r<sup>-</sup> mode is also different for the SSP and PPP polarization combinations. On the other hand, the SPS spectra display only the d<sup>-</sup> and r<sup>-</sup> mode. These differences are not a consequence of a different relative tilt angle of the alkyl chains with respect to the surface normal as it would be for SFG in the reflection geometry,<sup>42</sup> but are a consequence of the nonlinear light scattering geometry. Nonlinear light scattering theory predicts that for SF scattering each polarization combination has a different number of surface susceptibility elements that contribute to the scattered SF spectra with different weights (represented by form factor functions that are determined by scattering angle and droplet size<sup>38</sup>). As a result, the PPP spectra are often the most intense ones, because this polarization combination reports on all tensor elements of the surface susceptibility, which also appear with a larger magnitude.<sup>38,43</sup> They are also subject to some weakly dispersive interaction from D<sub>2</sub>O, as we observed before.<sup>44</sup> In contrast, here only the antisymmetric modes are visible in the SPS spectra, which is expected because SPS is the only polarization combination for which the β<sup>(2)</sup><sub>aca</sub> elements of the hyperpolarizability tensor are dominant. A molecular tilt angle ϕ away from the surface normal does reduce the overall intensity, because SFS is only reporting on molecular groups that have some kind of preferential alignment along the surface normal of an isotropic surface (see Supporting Information eq S5, just like in reflection mode SFG). We found previously<sup>38</sup> that the r<sup>-</sup> mode is sensitive to the tilt angle of the methyl group, while the r<sup>+</sup> mode is less sensitive, and the d<sup>+</sup> modes are not sensitive at all to the tilt angle. Thus, by calculating the different amplitude ratios<sup>38</sup> we can determine the average tilt angle ϕ of the terminal CH<sub>3</sub> group with respect to the droplet surface normal. Compared to other possible peak ratios, the r<sup>+</sup>/r<sup>-</sup> amplitude ratio of the SSP spectrum shows the highest sensitivity to the change of the tilt angle of the CH<sub>3</sub> group (see Supporting Information Figure S2).

Figure 2C shows a computation of the r<sup>+</sup>/r<sup>-</sup> amplitude ratio as a function of ϕ assuming a hyperpolarizability ratio<sup>40</sup> of 3.4 and a δ-distribution of tilt angles (blue line), as well as a broad Gaussian distribution (assuming an angular full width at half-maximum of 70°) of tilt angles (red line). Both functions for the orientational distribution thus represent two extremes of a surface structure: one highly ordered one and one highly disordered in terms of tilt angle. The experimental values found

for the  $r^+/r^-$  amplitude ratio from the fits in Figure 2A,B are 2.8 for 1-dodecanol and 3.0 for hexadecane. Comparing these values to the calculated lines, we find (assuming a  $\delta$ -function) that  $\phi_{C_{12OH}} = 33 \pm 5^\circ$  and  $\phi_{C_{16}} = 38 \pm 5^\circ$ . These values are both not far away from the value reported for a random distribution of tilt angles and do not necessarily report on an actual narrow tilt angle distribution.<sup>45</sup> For the broad Gaussian distribution, we find  $\phi_{C_{12OH}} = 49 \pm 17^\circ$  and  $\phi_{C_{16}} = 66 \pm 17^\circ$ . Because both tilt angle scenarios can describe the spectral data, it is likely that there is a broad distribution of tilt angles, as would be the case in a liquid phase. This agrees with the shape of spectra of Figure 2, which are clearly not representative of a crystalline-like film (which would have a negligible amount of  $d^+$  signal, as found for the 1-dodecanol/water interface<sup>14</sup>). The  $d^+/r^+$  ratios and the tilt angle analysis thus both indicate a broad distribution, which is in agreement with the interfacial layer being liquid-like. To further investigate the interaction of oil and alkanols, we vary the chain length of the alkanols and compare their alkyl structures as well as the oil chain structure using selective deuteration and make a comparison to the pure oil droplet/water interface.

**Chain Length Dependence.** Figure 3A shows SFS spectra of the C–H-stretch modes of different alkanols that are present at the interfaces of  $d_{34}$ -hexadecane droplets dispersed in  $D_2O$  with 1-dodecanol, 1-octanol, 1-hexanol, or 1-pentanol added to it. The spectra were recorded in the SSP polarization combination and normalized to the symmetric methyl stretch mode. Figure 3B shows the corresponding SF amplitudes, which were obtained by taking the square root of the integrated C–H spectra. The corresponding spectral changes for the hexadecane are shown in Figure 3C. These spectra were obtained by using deuterated alkanols and recorded in the PPP polarization combination. It can be seen that both the spectral shape and the intensity change with respect to pure  $n$ -hexadecane droplets in pure water (black line).

Figure 3 shows that the spectral shape (A) and amplitude (B) for 1-hexanol, 1-octanol, and 1-dodecanol are not changing much. Both results combined suggest that the interfacial density of the three longest chain alkanols is constant and adding  $CH_2$  pairs to the backbone of the alkyl chain does not contribute to the SFS signal. The spectrum of 1-pentanol has a reduced amplitude but an identical shape, which indicates a reduced surface coverage. In theory, it could also indicate an identical surface density but with a molecular orientation that is more parallel to the interface. This explanation of the lower amplitude does not agree with the fact that 1-pentanol is the most hydrophilic of the alkanols studied here (see Figure 1). We have also tried to measure the 1-butanol spectrum but we were not able to detect any SF signal in the C–H stretch region. This agrees with earlier studies<sup>37,46</sup> that have shown that at least four carbon atoms are needed to render a molecule hydrophobic and SFS visible.

Figure 3C shows that in contrast to the alkanols, the hexadecane does have a different SF spectrum for each different interface. The spectrum of pure oil droplets in pure  $D_2O$  contains spectral features that match with alkane chains that are predominantly oriented along the interfacial plane and not with alkane chains that are perpendicularly oriented.<sup>43,44</sup> Molecular dynamics simulations point to a similar conclusion.<sup>47</sup> We see from Figure 3C that the shorter alkanols lead to a bigger change in the oil structure: The overall intensity increases, the  $d^+/r^+$  ratio becomes bigger and more antisymmetric stretch mode character is observed in the spectra (which is why we chose to

plot the PPP polarization combination). Thus, it is likely that for a bigger mismatch in chain length more defects appear in the alkane chains, which results in a larger overall number of chain segments that are tilted toward the surface normal. That the 1-dodecanol covered hexadecane droplets differ less from the pure oil spectra than the 1-hexanol covered droplets indicates that the oil phase is shielded better by longer chain alkanols than by shorter chain alkanols as expected. This implies that some part of the longer alkanol chains will have to follow the more parallel structure of the oil chains.

Having thus determined that the alkanols seem to form a liquid-like layer on the surface of the oil droplets and that they induce structural changes in the oil phase, we now turn to estimating the surface density in a more precise way. To this end, we use 1-hexanol, which is soluble in both water and hexadecane.

**Concentration Dependence: Isotherm and Water Structure.** In order to determine the interfacial density of 1-hexanol, we collected SFS spectra of  $d_{34}$ -hexadecane droplets in water that were all prepared in the same emulsification procedure, and to which different amounts of aqueous 1-hexanol solution were added (following the procedure described in ref 39). Using this procedure, the droplet concentration and average radius remains constant.

Figure 4 shows the amplitude of the total C–H stretch mode signal of 1-hexanol that is adsorbed on the surface of  $d_{34}$ -

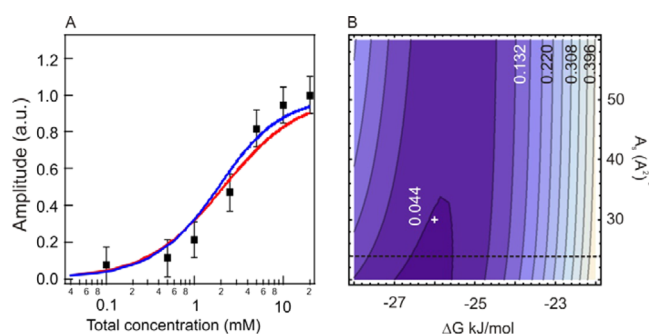


**Figure 4.** Isotherm of hexanol. (A) Amplitude of the C–H stretch modes of 1-hexanol that is adsorbed on the surface of  $d_{34}$ -hexadecane droplets ( $R = 163 \pm 24$  nm). The SFS spectra were recorded in the PPP polarization combination and with a scattering angle of  $\theta = 57^\circ$  (measured in air). Two different fits are shown: a fit to the Langmuir equation (red) and a fit to the modified Langmuir equation (blue).<sup>48</sup> The fit parameters are  $\Delta G = -24.7$  kJ/mol (Langmuir model, red) and  $\Delta G = -26.3$  kJ/mol;  $R = 139$  nm;  $A_s = 30$   $\text{\AA}^2$  (modified Langmuir model, blue). (B) contour plot of the squares of the difference between the modified Langmuir fit and the experiment data for  $R = 139$  nm. The white plus sign indicates the parameters of the blue curve in (A). The dashed line indicates the limiting surface area based on the increase in SFS amplitude.

hexadecane droplets (black squares) in water. The spectra from which these points are derived were recorded in PPP polarization (as the relative error is the smallest) and they did not change much in spectral shape. Because of this, the SF amplitude can be considered proportional to the surface density of adsorbed molecules ( $N$ ), which can be described using the Langmuir adsorption equation, and Eienthal's modified Langmuir equation.<sup>48</sup> Taking the maximum achievable surface density as  $N_{\text{max}}$  we can then describe the amplitude as being proportional to the ratio  $N/N_{\text{max}}$ . If the maximum surface site

concentration is much smaller than the total concentration of 1-hexanol ( $c$ ) we can write

$$\frac{N}{N_{\max}} = \frac{Kc}{(c^{\ominus} + Kc)} \text{ with } K = e^{-\Delta G/R_g T} \quad (1)$$

It should be noted that the unit of  $N$  and  $N_{\max}$  is mol/L, which is to be interpreted as the number of molecules adsorbed on the surface expressed per volume unit.  $K$  is the equilibrium constant,  $R_g$  is the gas constant ( $R_g = 8.31$  J/mol·K with a subscript  $g$  to distinguish it from the radius of the droplet  $R$ ),  $T$  is the temperature in K,  $\Delta G$  is the free energy of surface adsorption in kJ/mol, and  $c^{\ominus}$  is the molar concentration of water (55.5 mol/L). In this case,  $\Delta G$  is the only fitting parameter. For the case that a significant number of 1-hexanol molecules are depleted from the solution, we can use Eisenthal's modified Langmuir model. This model is expected to be closer to reality since a 1 vol % solution of 163 nm radius droplets can accommodate  $\sim 1.5$  mM of 1-hexanol on its surface, using a projected surface area per molecule of  $20 \text{ \AA}^2$ , which is close to the projected area of an alkanol molecule in a packed alkanol layer ( $18.7\text{--}21 \text{ \AA}^2$ ).<sup>49</sup> We then use

$$\frac{N}{N_{\max}} = \frac{1}{2N_{\max}} \left\{ c + N_{\max} + \frac{c^{\ominus}}{K} - \sqrt{\left( c + N_{\max} + \frac{c^{\ominus}}{K} \right)^2 - 4cN_{\max}} \right\} \quad (2)$$

which uses the same parameters as eq 1. For this case,  $N_{\max}$  and  $\Delta G$  are both fitting parameters.  $N_{\max}$  can further be expressed as  $N_{\max} = (3\phi V_{\text{tot}} 10^{-3}) / (RN_{\text{av}}A_s)$  where  $\phi$  is the volume fraction of oil droplets,  $V_{\text{tot}}$  is the total volume of the emulsion, and  $R$  is the average (hydrodynamic) droplet radius. We use  $R = 163 \pm 24$  nm, which is the range of values obtained from DLS measurements. In the fitting procedure, we let  $R$  free to vary between 139 and 187 nm.  $N_{\text{av}}$  is Avogadro's number ( $6.02 \times 10^{23} \text{ mol}^{-1}$ ) and  $A_s$  is the projected minimum surface area per 1-hexanol molecule. Note that for both models, it is assumed that the probability for adsorption or adsorption energy is independent of the surface occupation or structure, that is, it is assumed to be an ideal gas. Figure 4A shows the obtained fits for both models. The fit values are  $\Delta G = -24.7$  kJ/mol (Langmuir model, red curve) and  $R = 139$  nm,  $\Delta G = -26.3$  kJ/mol, and  $A_s = 30 \text{ \AA}^2$  (modified Langmuir model, blue curve). Figure 4B shows a contour plot of the square of the difference between the modified Langmuir fit (using  $R = 139$  nm) and the data points. The white plus sign indicates the parameters of the blue curve. It can be seen that there is a greater relative sensitivity to  $\Delta G$  than to  $A_s$ . Nevertheless, the data does show that it is reasonable to expect that the projected area per 1-hexanol molecule is in the range of  $20\text{--}34 \text{ \AA}^2$ , with  $\Delta G$  values in the range of  $-25.6 > \Delta G > -27.0$  kJ/mol. In addition, the range of  $A_s$  can be narrowed down by noting that the SFS amplitude (and hence the surface density) cannot exceed the maximum amount that could be present on the surface for the lowest concentration (i.e., all hexanol molecules present in the system) multiplied by the relative amplitude increase (13.6) in going from the lowest (100  $\mu\text{M}$ ) to the highest concentration (20 mM). For the experimental average of  $R = 163$  nm, we arrive at a lower limit of  $24 \text{ \AA}^2$  for  $A_s$ , such that  $A_s = 29 \pm 5 \text{ \AA}^2$ . The projected areas agree qualitatively with the SFS spectrum of the alkyl chains of 1-hexanol, which shows a fairly ordered alkyl chain ( $d^+/r^+ = 0.7$ ) that is also close to what is found with SFG studies on the planar interface of 1-hexanol liquid in contact with air,<sup>11,16</sup> and temperature-dependent surface

tension measurements on the 1-hexanol/hexadecane/water interface<sup>50</sup> that reported areas of  $28\text{--}70 \text{ \AA}^2$  per molecule with a  $\Delta G$  value of  $-23.3$  kJ/mol. In addition, the value found for  $\Delta G$  is much larger than that found for the transfer of 1-hexanol from water to hexadecane which is  $-9.08$  kJ/mol<sup>4</sup>. Also, based on Figure 3A,B, because the SF spectra for the alkanols are very similar in both shape and intensity, we can expect that the surface densities of 1-octanol and 1-dodecanol are comparable.

We thus see that the alkanols form liquid-like films on the hexadecane droplet interface that influence the oil structure. Shorter alkanol chains lead to bigger changes in the oil structure. Next, we determine if the water structure is also influenced by the alkanols. To investigate this, we use again 1-hexanol and probe the water structure with second harmonic scattering.<sup>51</sup>

**Interfacial Water Alignment.** The interfacial water around our nanoscopic droplets can be measured with second harmonic<sup>31</sup> scattering,<sup>27,32–34</sup> a process that occurs only in noncentrosymmetric materials. As shown by Eisenthal and co-workers,<sup>31</sup> the SH signal reports on the difference in dynamic orientational directionality of the water molecules in the interfacial region compared to the orientational directionality in the bulk solution.<sup>31,35–37</sup> The reason for that is that for a nonresonant process the signal depends quadratically on the number density of each component that is both dipolar and present in the noncentrosymmetric interfacial region. Because water has the largest hyperpolarizability (which also contributes quadratically) and because it greatly outnumbers the other species, the SHS signal reports primarily on the water orientation. Here, the change in directionality is induced only by interactions between the water and the 1-hexanol molecules. Charge effects can be excluded because all compounds are neutral. Indeed, the zeta potential of the droplets is verified to be constant ( $\zeta = -60 \pm 6$  mV). For a discussion about the origin of the large electrokinetic mobility and our explanation as originating from charge transfer effects in water, we refer to ref 52. Figure 5A displays the SHS intensity obtained at a scattering angle ( $\theta$ ) of  $35^\circ$  using the PPP polarization combination (i.e., all beams are polarized in the horizontal scattering plane), and around the angle of maximum intensity<sup>53</sup> for emulsions containing different concentrations of 1-hexanol. The above derived projected average surface area for each hexanol molecule is plotted on the top axis. The measured intensity was corrected for hyper-Rayleigh scattering from the same solution without droplets and then divided by the hyper-Rayleigh scattering intensity in PPP polarization of pure water for normalization purposes (following ref 54).

It can be seen that the interfacial SHS intensity of hexadecane droplets in water is approximately three times the value of the SHS signal of pure water. That means that in absence of 1-hexanol orientational directionality of water is increased by the presence of oil droplets. This oriented water has a small majority of H atoms pointing toward the surface.<sup>23,55</sup> Upon adding 1-hexanol to the emulsion, a reduction of the directionality of water along the surface normal is observed. This reduction can be explained by additional H-bonding interaction that occurs between the hydroxyl group of the added hexanol molecule and the water. The  $-\text{CH}_2\text{OH}$  group is sticking into the water phase and only H-bonds with a water molecule that has its O atom pointing toward the interfacial plane (see Figure 5B; note that this illustration purely serves to highlight the changing directionality

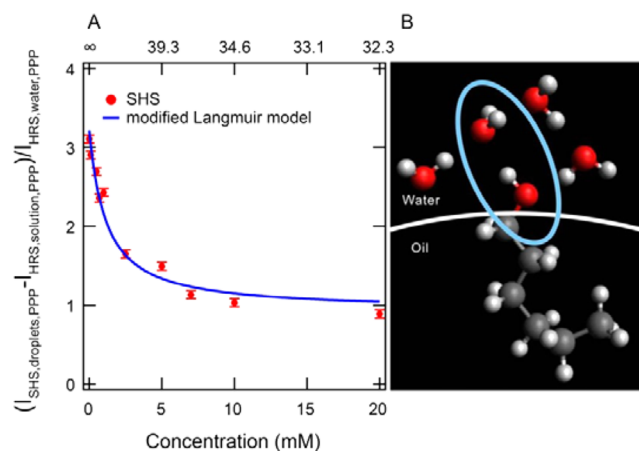


**Figure 5.** Water alignment. (A) SHS intensities for hexadecane droplets in water prepared with different amounts of 1-hexanol. The PPP intensity was measured at the maximum scattering angle ( $\theta = 35^\circ$ ), corrected for hyper-Rayleigh scattering and normalized by the PPP signal of pure water. It can be seen that relative to a pure oil droplet/water interface the orientational directionality of water is reduced when more 1-hexanol is present at the interface. The blue line represents the function  $(A - B(N/N_{\text{max}}))^2$  with  $A = 1.79$  and  $B = 0.83$ . The values used for  $(N/N_{\text{max}})$  originate from the fit of the data in Figure 4A. (B) Illustration of the effect of the hexanol headgroup on the interfacial water structure. The zeta potential of all droplets is the same,  $-60 \pm 6$  mV.

of H-bonding). When the concentration is increased and more 1-hexanol molecules are present at the interface, a larger number of water molecules will be reoriented, which means that the net orientational directionality of water molecules will be reduced, thereby decreasing the SHS signal. Because one 1-hexanol molecule forms only one H-bond, there should be a linear relationship between the number of 1-hexanol molecules that are present at the interface and the reduction in the number of water molecules that contribute to the SHS signal. If this is the case, we can use the outcome of the modified Langmuir model fitting of the SFS data in Figure 4A to fit the data in Figure 5.  $N/N_{\text{max}}$  should also represent the number of water molecules that have been reoriented by H-bonding. The SHS intensity should then be described by a function of the form  $[A - B(N/N_{\text{max}})]^2$  which, as can be seen from Figure 5A, is indeed the case. The parameters  $A$  and  $B$  have no physical meaning other than to represent the geometry of the experiment. Thus, the SHS measurement of water and the SFS measurement of 1-hexanol are in good agreement with each other.

**The Interfacial Structure.** Here we will first discuss the interfacial structure of the water/alkanol/hexadecane interface and then make a comparison to the alkanol/air and the water/alkanol/air interface.

The alkanols studied in the oil droplet/water system form a transition layer between a relatively ordered structure on the water side of the interface, which is determined by the H-bonding network of water that allows only certain configurations of the  $-\text{OH}$  groups to a relatively ordered structure of mostly parallel oriented oil molecules, as present at the pure hexadecane/water interface.<sup>43,44,47</sup> The longer chain 1-dodecanol forms liquid-like films with a fairly high degree of chain order that is visible in the SFS spectra ( $d^+/r^+ < 1$ ). Shortening the alkyl chain length, we observe that the SFS spectra for  $\text{C}_6$ – $\text{C}_{12}$  are identical in shape and amplitude. Thus, the surface

density for  $\text{C}_6$ – $\text{C}_{12}$  is comparable. In contrast, 1-pentanol is much less surface active and 1-butanol was not detected in the SFS experiments. We also see that the hexadecane alkyl chains are strongly influenced by the alkanol monolayer. The oil alkyl chains appear to intercalate with the alkanol alkyl chains, as their SF spectra change when alkanols are added to the interfacial region and they become more distorted in their conformation by shorter alkanols than by the longer ones. SFS measurements and subsequent fitting with the modified Langmuir model on a concentration series of 1-hexanol show that 1-hexanol films with a projected molecular area of  $29 \pm 5 \text{ \AA}^2$  are formed. The corresponding free energy of adsorption is in the range of  $-25.7 > \Delta G > -27.0$  kJ/mol. SHS measurements that report on the directionality of interfacial water show that the interfacial water restructures as well, whereby it is seen that the orientational directionality of the interfacial water is reduced. The reduction of SHS signal is proportional to the formation of one H-bond per 1-hexanol molecule.

Starting at the water side, the H-bonding network and the high chain density result in a large degree of order between the  $\text{C}_n\text{OH}$  groups. Moving toward the oil phase the chance of forming a gauche defect increases.<sup>16</sup> For 1-dodecanol, we see that the distribution of orientational angles of the terminal  $\text{CH}_3$  group with respect to the interfacial normal is broad and close to a random distribution. For 1-dodecanol, the oil is also minimally perturbed compared to the other shorter chain alkanols. This behavior can be explained by a structure that consists of alkyl chains of 1-dodecanol molecules that bend from a nearly perpendicular orientation (imposed by the water) into one that is more parallel (imposed by the oil), following the structure of the oil surface. The shorter alkyl chains will do the same thing on the water side but are not long enough to make a smooth transition to the more parallel oriented alkyl chain orientation of the oil phase. Aided by thermal fluctuations, they will perturb the oil phase more (as seen in Figure 3). If the chains would not bend toward the interface but form structures of more perpendicular oriented chains, we would not expect the result of Figure 3A,C. Namely unbent alkanols would distort the oil molecules independent of chain length and would also have different  $d^+/r^+$  ratios.<sup>25</sup> Figure 6 shows an illustration of possible structures that agree with the above considerations. To arrive at this particular illustration, we have taken into consideration that the end methyl groups are most likely SF visible as they are thermally free to adopt any

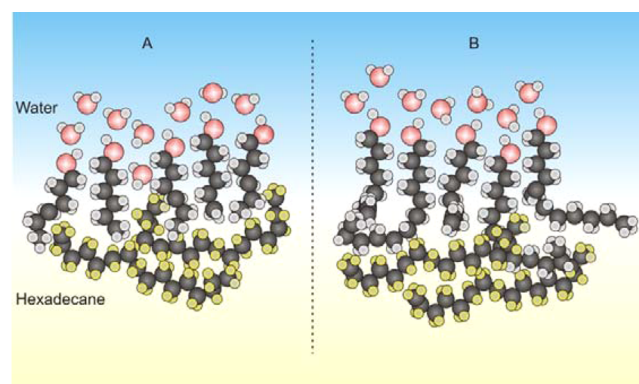


**Figure 6.** Illustration of possible surface structures of 1-hexanol (A) and 1-dodecanol (B) at the hexadecane droplet/water interface.

conformations (which is clear from the analysis in Figure 2C). For the methylene groups, we consider that only the CH<sub>2</sub> groups that are neither even in number and oriented perpendicular to the interface nor parallel oriented to the interface are SF active.

**A Comparison to the Alkanol/Water and Alkanol/Air Interface.** The water/dodecanol/air interface<sup>10,12–15</sup> is characterized by alkyl chains with very few gauche–trans defects (reporting a d<sup>+</sup>/r<sup>+</sup> ratio for 1-dodecanol of <0.1 for the solid phase and 0.3 for the liquid phase) and an almost perpendicular chain orientation with respect to the interface. Here, the layer consists of a relatively tightly packed structure of alkyl chains with projected areas of 21.5 Å<sup>2</sup> per molecule in the solid phase (below 38.5 °C) and 23.8 Å<sup>2</sup> (ref 14, ellipsometry and SFG) or 25 Å<sup>2</sup> (XRD, ref 6) for the liquid phase. The difference with the oil/water interface is the absence of a hydrophobic condensed phase that participates in dispersive interactions. In absence of a liquid oil phase, the dispersive attraction between the alkyl chains results in a more tightly packed layer.

SFG measurements in reflection mode from the C<sub>1</sub>OH–C<sub>8</sub>OH/air interface showed that the alkanol alkyl chains have as well a preferential orientation toward the air<sup>11,16</sup> but with a very broad orientational distribution, and a larger amount of gauche trans disorder that increases with the chain length. For 1-hexanol/air, the reported d<sup>+</sup>/r<sup>+</sup> ratio is approximately ~0.6 and for 1-octanol it is approximately 0.9. In this case, the H-bonding interaction is different (namely between the alkanols only), which likely results in a different packing and thus different chain conformations.

The planar oil/water interface of hexadecane/1-hexanol/water was studied with temperature-dependent surface tension measurements.<sup>50</sup> Fits with various models reported on a projected surface area of 28–70 Å<sup>2</sup>. Anomalies in the temperature dependence of the surface tension and the relative insensitivity of Gibbs free energies on chain length were attributed to hexanol induced structural rearrangement of the water at the interface.

Alkanols with longer chain lengths (C<sub>20</sub>–C<sub>30</sub>) were studied with X-ray diffraction on the hexane/water interface. A typical projected surface area of 23 Å<sup>2</sup> was retrieved for these liquid-like layers. It was also found that disorder increases from the headgroup downward and that for every five alkanol chains there is one intercalating hexane molecule. In addition there is also some water in the top of the surface layer.<sup>49</sup>

Comparing our data to the above studies, we see that there is qualitative agreement: the changes in the water structure corroborate the anomalies in the temperature-dependent surface tension measurements, the projected surface areas and free energy of adsorption are in the same range as the reported XRD and surface tension measurements, and the amount of alkyl chain disorder (as empirically reported on by the d<sup>+</sup>/r<sup>+</sup> ratio's) is in between that of liquid alkanols and “solid” alkanols at the air/water interface. These differences are probably caused by the presence/absence of oil and water that provide constraints on the possible geometries that can be adopted by the alkanols. Compared to hexadecane droplets dispersed in water and covered with charged surfactants of dodecyltrimethylammonium bromide (DTAB) and sodium dodecyl sulfate (SDS),<sup>51</sup> we find that there are clear differences in surface density (which is much higher in the case of the neutral alkanols) and surface oil and surface water structure. While all surfactants studied change in the water structure, they do so differently. The same is true for the oil phase. Thus, by

spectroscopically measuring the oil, the surfactant, and the water on these nanoscopic droplets we see that the specific chemical interactions are highly relevant to the interfacial properties rather than just the concept of geometrical packing.

## CONCLUSIONS

We have obtained molecular level insight into the molecular structural aspects of the transition from a hydrophobic to an aqueous phase, using a dispersion of ~100 nm hexadecane droplets in water that also contains 1-pentanol, 1-hexanol, 1-octanol, or 1-dodecanol. We examined the alkyl chain conformation of the alkanols and the oil, the surface density of the alkanols and the structural changes imposed on the water using a combination of second harmonic and sum frequency scattering. The hexadecane/1-dodecanol/water interface has a chain conformation that represents that of a fluid layer with a wide distribution of tilt angles of the terminal CH<sub>3</sub> groups. Changing the chain length of the alkanol, the alkanol alkyl chains adopt a conformation that generates indistinguishable SF spectra for pentanol to dodecanol, whereby the alkanols with chain length longer than 6 C atoms all form films with comparable chain densities. In contrast, the alkyl chains of the oil phase are relatively more distorted with respect to the pure oil/water interface as the alkyl chain length of the alkanol decreases. The surface density was determined more accurately by means of an SFS isotherm of 1-hexanol, which generated a projected surface density of 29 ± 5 Å<sup>2</sup> and a free energy of adsorption of ΔG = -26.3 ± 0.7 kJ/mol. With increasing 1-hexanol density the interfacial water structure loses its initial orientational alignment in a way that matches with the added number of interfacial 1-hexanol molecules. The found conformations differ significantly from that reported on the alkanol/water and alkanol/air interface, which can be explained by the balance between dispersive and H-bonding interactions.

## MATERIALS AND METHODS

Hexadecane (C<sub>16</sub>H<sub>34</sub>, 99.8%, Sigma-Aldrich), d<sub>34</sub>-hexadecane (C<sub>16</sub>D<sub>34</sub>, 98% d, Cambridge Isotope), 1-pentanol (CH<sub>3</sub>(CH<sub>2</sub>)<sub>4</sub>OH, 99%, Acros), 1-pentanol-d<sub>11</sub>-ol (CD<sub>3</sub>(CD<sub>2</sub>)<sub>4</sub>OH, 98% d, Sigma-Aldrich), 1-hexanol (CH<sub>3</sub>(CH<sub>2</sub>)<sub>5</sub>OH, 99.5%, Sigma-Aldrich), 1-hexanol-d<sub>13</sub>-ol (CD<sub>3</sub>(CD<sub>2</sub>)<sub>5</sub>OH, 98% d, Sigma-Aldrich), 1-octanol (CH<sub>3</sub>(CH<sub>2</sub>)<sub>7</sub>OH, 99%, Sigma-Aldrich), 1-octanol-d<sub>17</sub>-ol (CD<sub>3</sub>(CD<sub>2</sub>)<sub>7</sub>OH, 98% d, Sigma-Aldrich), 1-dodecanol (CH<sub>3</sub>(CH<sub>2</sub>)<sub>11</sub>OH, 98%, Sigma-Aldrich), and 1-dodecanol-d<sub>25</sub>-ol (CD<sub>3</sub>(CD<sub>2</sub>)<sub>11</sub>OH, 98% d, Sigma-Aldrich) were used as received. All aqueous solutions were made with ultrapure water (H<sub>2</sub>O, Milli-Q UF plus, Millipore, Inc., electrical resistance of 18.2 MΩ cm; D<sub>2</sub>O 99.8% Armar, > 2 MΩ cm). Glassware was cleaned with a 1:3 H<sub>2</sub>O<sub>2</sub>/H<sub>2</sub>SO<sub>4</sub> solution after which it was thoroughly rinsed with ultrapure water (H<sub>2</sub>O, Milli-Q UF plus, Millipore, Inc., electrical resistance of 18.2 MΩ cm).

Dispersions of oil nanodroplets in water were prepared with 1 vol % (Figures 2 and 3) or 2 vol % (Figure 4) of *n*-hexadecane or d<sub>34</sub>-hexadecane in D<sub>2</sub>O for SFS and in H<sub>2</sub>O for SHS. The solutions were mixed with 5 mM alkanols for 4 min with a hand-held homogenizer (TH, OMNI International) and subsequently placed in an ultrasonic bath (35 kHz, 400 W, Bandelin) for the same duration. The resultant emulsions of alkanols except hexanol were directly used for SFS. A concentration of 5 mM is used in the study of the interfacial

structures of alkanols and oil (Figures 2 and 3). The resultant stock emulsion of hexanol was diluted to 1 vol % of hexadecane with a solution of alkanol in water to yield the desired alkanol concentration for SFS (0.1 vol % for SHS). For 1-hexanol a concentration series ranging from 0.1 to 20 mM was used for the isotherm study (Figures 4 and 5). The size distribution and zeta-potential of the nanodroplets were measured with dynamic light scattering and electrokinetic mobility measurements (Malvern ZS nanosizer). The nanodroplets were consistently found to have a mean hydrodynamic diameter in the range of 220–300 nm with a polydispersity index (PDI) of less than 0.3. All samples were stable for at least several weeks. All measurements were performed at 24 °C.

Second harmonic scattering measurements were performed, as previously described in detail,<sup>34</sup> using 190 fs laser pulses with a 200 kHz repetition rate. The input laser beams were centered at 1028 nm and polarized by a Glan-Taylor polarizer (GT10-B, Thorlabs). A zero-order half wave plate (WPH05M-1030) was used to control the polarization of the input pulses. The input pulses were then filtered (FEL0750, Thorlabs) and focused into a cylindrical glass sample cell (4.2 mm inner diameter, high precision cylindrical glass cuvettes, LS instruments) with a waist diameter of ~35 μm and a Rayleigh length of ~0.94 mm. The input pulse energy at the sample was set 0.25 μJ (incident laser power  $P = 50$  mW). The scattered SH light was filtered (ETS25/50, Chroma), polarized (GT10-A, Thorlabs), collected, collimated with a plano-convex lens ( $f = 5$  cm), and finally focused into a gated PMT (H7421-40, Hamamatsu). The detection angle was set at 35° with an acceptance angle of 11.4°. Data points were acquired with 20 × 1 s acquisition time and a gate width of 10 ns. The plotted data points represent the SHS signal corrected for the background hyper-Rayleigh scattering and normalized by the PPP signal of neat water

$$\frac{I(\theta = 35^\circ)_{\text{SHS, droplets, PPP}} - I(\theta = 35^\circ)_{\text{HRS, solutions, PPP}}}{I(\theta = 35^\circ)_{\text{HRS, water, PPP}}}$$

The reproducibility of the SHS measurements is in the range of 1–2%.

Vibrational SFS spectra were measured using the same SFS setup as previously described in refs 56 and 57. Briefly, broadband IR laser pulses centered at 2900 cm<sup>-1</sup> (fwhm = 120 cm<sup>-1</sup>) and visible (vis) pulses at 800 nm (fwhm = 12 cm<sup>-1</sup>) at a repetition rate of 1 kHz were used as the input beams. The input laser beams were focused and overlapped under an angle of 15° (as measured in air) in a sample cuvette with a path length of 200 μm. The scattered SF light was collimated using a plano-convex lens ( $f = 15$  mm, Thorlabs LA1540-B) at a scattering angle of 57° (as measured in air) and passed through two short-pass filters (third Millennium, 3RD770SP). The SF light was spectrally dispersed with a monochromator (Acton, SpectraPro 2300i) and detected with an intensified charge-coupled device camera (Princeton Instruments, PI-Max3) using a gate width of 10 ns. The acquisition time for a single spectrum was set 150 s. A Glan-Taylor prism (Thorlabs, GT15-B), a half-wave plate (EKSMA, 460-4215), and a polarizing beam splitter cube (CVI, PBS-800-050), and two BaF<sub>2</sub> wire grid polarizers (Thorlabs, WP25H-B) were used to control the polarization of the SF, vis, and IR beams, respectively. The SFG spectrum obtained in the reflection geometry from a z-cut quartz crystal was used to normalize all the SFS spectra of tested samples. Concentration series were measured against a reference sample that was inserted between every other

measurement to detect and correct for possible fluctuations during the course of the experiment. The  $d^+/r^+$  and  $r^+/r^-$  amplitude ratios were obtained from a global fitting applied to the SFS spectra in which the weak nonresonant background was taken into account by using a measured SFS signal from an all-deuterated sample. This was done because the nonresonant background varied per sample and polarization direction. More details can be found in the Supporting Information and in ref 44.

## ■ ASSOCIATED CONTENT

### 📄 Supporting Information

More details about the spectral fitting (S1) and the determination of the orientation of terminal methyl groups (S2). The Supporting Information is available free of charge on the ACS Publications website at DOI: 10.1021/acs.jpcc.5b04904.

## ■ AUTHOR INFORMATION

### Corresponding Author

\*E-mail: sylvie.roke@epfl.ch.

### Notes

The authors declare no competing financial interest.

## ■ ACKNOWLEDGMENTS

This work is supported by the Julia Jacobi Foundation, the Swiss National Science Foundation (Grant 200021\_140472), the European Research Council (Grant 240556).

## ■ REFERENCES

- (1) Pockels, A. Surface Tension. *Nature* **1891**, 43, 437.
- (2) Langmuir, I. The Constitution and Fundamental Properties of Solids and Liquids. II. Liquids. *J. Am. Chem. Soc.* **1917**, 39, 1848–1906.
- (3) Harkins, W. D.; Davies, E. C. H.; Clark, G. L. The Orientation of Molecules in the Surfaces of Liquids, the Energy Relations at Surfaces, Solubility, Adsorption, Emulsification, Molecular Association, and the Effect of Acids and Bases on Interfacial Tension. *J. Am. Chem. Soc.* **1917**, 39, 354–364.
- (4) Abraham, M. H.; Whiting, G. S.; Fuchs, R.; Chambers, E. J. Thermodynamics of Solute Transfer from Water to Hexadecane. *J. Chem. Soc., Perkin Trans. 2* **1990**, 291–300.
- (5) Als-Nielsen, J.; McMorrow, D. *Elements of Modern X-Ray Physics*; Wiley & Sons: Hoboken, NJ, 2001.
- (6) Berge, B.; Konovalov, O.; Lajzerowicz, J.; Renault, A.; Rieu, J. P.; Vallade, M.; Alsnielsen, J.; Grubel, G.; Legrand, J. F. Melting of Short 1-Alcohol Monolayers on Water - Thermodynamics and X-Ray-Scattering Studies. *Phys. Rev. Lett.* **1994**, 73, 1652–1655.
- (7) Bain, C. D. Sum-Frequency Vibrational Spectroscopy of the Solid/Liquid Interface. *J. Chem. Soc., Faraday Trans.* **1995**, 91, 1281–1296.
- (8) Richmond, G. L. Structure and Bonding of Molecules at Aqueous Surfaces. *Annu. Rev. Phys. Chem.* **2001**, 52, 357–389.
- (9) Roke, S. Nonlinear Optical Spectroscopy of Soft Matter Interfaces. *ChemPhysChem* **2009**, 10, 1380–1388.
- (10) Seifler, G. A.; Du, Q.; Miranda, P. B.; Shen, Y. R. Surface Crystallization of Liquid n-Alkanes and Alcohol Monolayers Studied by Surface Vibrational Spectroscopy. *Chem. Phys. Lett.* **1995**, 235, 347–354.
- (11) Lu, R.; Gan, W.; Wu, B.; Zhang, Z.; Guo, Y.; Wang, H. C-H Stretching Vibrations of Methyl, Methylene and Methine Groups at the Vapor/Alcohol (N=1–8) Interfaces. *J. Phys. Chem. B* **2005**, 109, 14118–14129.
- (12) Bell, G. R.; Bain, C. D.; Ward, R. N. Sum-Frequency Vibrational Spectroscopy of Soluble Surfactants at the Air/Water Interface. *J. Chem. Soc., Faraday Trans.* **1996**, 92, 515–523.



- (13) Braun, R.; Casson, B. D.; Bain, C. D. A Sum-Frequency Study of the 2-Dimensional Phase-Transition in a Monolayer of Undecanol on Water. *Chem. Phys. Lett.* **1995**, *245*, 326–334.
- (14) Casson, B. D.; Braun, R.; Bain, C. D. Phase Transitions in Monolayers of Medium-Chain Alcohols on Water Studied by Sum-Frequency Spectroscopy and Ellipsometry. *Faraday Discuss.* **1996**, *104*, 209–229.
- (15) Tyrode, E.; Johnson, C. M.; Kumpulainen, A.; Rutland, M. W.; Claesson, P. M. Hydration State of Nonionic Surfactant Monolayers at the Liquid/Vapor Interface: Structure Determination by Vibrational Sum Frequency Spectroscopy. *J. Am. Chem. Soc.* **2005**, *127*, 16848–16859.
- (16) Stanners, C. D.; Du, Q.; Chin, R. P.; Cremer, P.; Somorjai, G. A.; Shen, Y. R. Polar Ordering at the Liquid-Vapor Interface of n-Alcohols (C<sub>1</sub>–C<sub>8</sub>). *Chem. Phys. Lett.* **1995**, *232*, 407–413.
- (17) Knock, M. M.; Bell, G. R.; Hill, E. K.; Turner, H. J.; Bain, C. D. Sum-Frequency Spectroscopy of Surfactant Monolayers at the Oil-Water Interface. *J. Phys. Chem. B* **2003**, *107*, 10801–10814.
- (18) Delcerro, C.; Jameson, G. J. The Behavior of Pentane, Hexane, and Heptane on Water. *J. Colloid Interface Sci.* **1980**, *78*, 362–375.
- (19) Goebel, A. K.; Lunkenheimer, K. Interfacial Tension of the Water/n-Alkane Interface. *Langmuir* **1997**, *13*, 369–372.
- (20) Gragson, D. E.; McCarty, B. M.; Richmond, G. L. Ordering of Interfacial Water Molecules at the Charged Air/Water Interface Observed by Vibrational Sum Frequency Generation. *J. Am. Chem. Soc.* **1997**, *119*, 6144–6152.
- (21) Scatena, L. F.; Brown, M. G.; Richmond, G. L. Water at Hydrophobic Surfaces: Weak Hydrogen Bonding and Strong Orientation Effects. *Science* **2001**, *292*, 908–912.
- (22) Brown, M.; Walker, D.; Raymond, E.; Richmond, G. Vibrational Sum-Frequency Spectroscopy of Alkane/Water Interfaces: Experiment and Theoretical Simulation. *J. Phys. Chem. B* **2003**, *107*, 237–244.
- (23) Strazdaite, S.; Versluis, J.; Backus, E. H. G.; Bakker, H. J. Enhanced Ordering of Water at Hydrophobic Surfaces. *J. Chem. Phys.* **2014**, *140*, 054711.
- (24) Guyot-Sionnest, P.; Hunt, J. H.; Shen, Y. R. Sum-Frequency Vibrational Spectroscopy of a Langmuir Film: Study of Molecular Orientation of a Two-Dimensional System. *Phys. Rev. Lett.* **1987**, *59*, 1597–1600.
- (25) Esenturk, O.; Walker, R. A. Surface Vibrational Structure at Alkane Liquid/Vapor Interfaces. *J. Chem. Phys.* **2006**, *125*, 174701–174712.
- (26) Tyrode, E.; Hedberg, J. A Comparative Study of the CD and CH Stretching Spectral Regions of Typical Surfactants Systems Using VSFS: Orientation Analysis of the Terminal CH<sub>3</sub> and CD<sub>3</sub> Groups. *J. Phys. Chem. C* **2012**, *116*, 1080–1091.
- (27) Wang, H.; Yan, E. C. Y.; Borguet, E.; Eienthal, K. B. Second Harmonic Generation from the Surface of Centrosymmetric Particles in Bulk Solution. *Chem. Phys. Lett.* **1996**, *259*, 15–20.
- (28) Eienthal, K. B. Second Harmonic Spectroscopy of Aqueous Nano- and Microparticle Interfaces. *Chem. Rev.* **2006**, *106*, 1462–1477.
- (29) Roke, S.; Gonella, G. Nonlinear Light Scattering and Spectroscopy of Particles and Droplets in Liquids. *Annu. Rev. Phys. Chem.* **2012**, *63*, 353–378.
- (30) Roke, S.; Roeterdink, W. G.; Wijnhoven, J. E. G. J.; Petukhov, A. V.; Kleyn, A. W.; Bonn, M. Vibrational Sum Frequency Scattering from a Sub-Micron Suspension. *Phys. Rev. Lett.* **2003**, *91*, 258302–258302.
- (31) Ong, S.; Zhao, X.; Eienthal, K. B. Polarization of Water Molecules at a Charged Interface: Second Harmonic Studies of the Silica/Water Interface. *Chem. Phys. Lett.* **1992**, *191*, 327–335.
- (32) Yan, E. C. Y.; Liu, Y.; Eienthal, K. B. New Method for Determination of Surface Potential of Microscopic Particles by Second Harmonic Generation. *J. Phys. Chem. B* **1998**, *102*, 6331–6336.
- (33) Schurer, B.; Hoffmann, M.; Wunderlich, S.; Harnau, L.; Peschel, U.; Ballauff, M.; Peukert, W. Second Harmonic Light Scattering from Spherical Polyelectrolyte Brushes. *J. Phys. Chem. C* **2011**, *115*, 18302–18309.
- (34) Gomopoulos, N.; Lütgebaucks, C.; Sun, Q.; Macias-Romero, C.; Roke, S. Label-Free Second Harmonic and Hyper Rayleigh Scattering with High Efficiency. *Opt. Express* **2013**, *21*, 815–821.
- (35) Petersen, P. B.; Saykally, R. J. Probing the Interfacial Structure of Aqueous Electrolytes with Femtosecond Second Harmonic Generation Spectroscopy. *J. Phys. Chem. B* **2006**, *110*, 14060–14073.
- (36) Jena, K. C.; Covert, P. A.; Hore, D. K. The Effect of Salt on the Water Structure at a Charged Solid Surface: Differentiating Second- and Third-order Nonlinear Contributions. *J. Phys. Chem. Lett.* **2011**, *2*, 1056–1061.
- (37) Scheu, R.; Chen, Y.; Subinya, M.; Roke, S. Stern Layer Formation Induced by Hydrophobic Interactions: A Molecular Level Study. *J. Am. Chem. Soc.* **2013**, *135*, 19330–19335.
- (38) de Beer, A. G. F.; Roke, S. Obtaining Molecular Orientation from Second Harmonic and Sum Frequency Scattering Experiments: Angular Distribution and Polarization Dependence. *J. Chem. Phys.* **2010**, *132*, 234702–234708.
- (39) de Aguiar, H. B.; de Beer, A. G. F.; Strader, M. L.; Roke, S. The Interfacial Tension of Nanoscopic Oil Droplets in Water Is Hardly Affected by SDS Surfactant. *J. Am. Chem. Soc.* **2010**, *132*, 2122–2123.
- (40) Wang, H. F.; Gan, W.; Lu, R.; Rao, Y.; Wu, B. H. Quantitative Spectral and Orientational Analysis in Surface Sum Frequency Generation Vibrational Spectroscopy (SFG-VS). *Int. Rev. Phys. Chem.* **2005**, *24*, 191–256.
- (41) Ward, R. N.; Duffy, D. C.; Davies, P. B.; Bain, C. D. Sum-Frequency Spectroscopy of Surfactants Adsorbed at a Flat Hydrophobic Surface. *J. Phys. Chem.* **1994**, *98*, 8536–8542.
- (42) Lambert, A. G.; Davies, P. B.; Neivandt, D. J. Implementing the Theory of Sum Frequency Generation Vibrational Spectroscopy: A Tutorial Review. *Appl. Spectrosc. Rev.* **2005**, *40*, 103–144.
- (43) Vácha, R.; Roke, S. Sodium Dodecyl Sulfate at Water-Hydrophobic Interfaces: A Simulation Study. *J. Phys. Chem. B* **2012**, *116*, 11936–11942.
- (44) de Aguiar, H. B.; Strader, M. L.; de Beer, A. G. F.; Roke, S. Surface Structure of SDS Surfactant and Oil at the Oil-in-Water Droplet Liquid/Liquid Interface: A Manifestation of a Non-Equilibrium Surface State. *J. Phys. Chem. B* **2011**, *115*, 2970–2978.
- (45) Simpson, G. J.; Rowlen, K. L. An SHG Magic Angle: Dependence of Second Harmonic Generation Orientation Measurements on the Width of the Orientation Distribution. *J. Am. Chem. Soc.* **1999**, *121*, 2635–2636.
- (46) Davis, J. G.; Gierszal, K. P.; Wang, P.; Ben-Amotz, D. Water Structural Transformation at Molecular Hydrophobic Interfaces. *Nature* **2012**, *491*, 582–585.
- (47) Rivera, J. L.; McCabe, C.; Cummings, P. T. Molecular Simulations of Liquid-Liquid Interfacial Properties: Water–n-Alkane and Water–Methanol–n-Alkane Systems. *Phys. Rev. E: Stat. Phys., Plasmas, Fluids, Relat. Interdiscip. Top.* **2003**, *67*, 011603.
- (48) Wang, H. F.; Yan, E. C. Y.; Liu, Y.; Eienthal, K. B. Energetics and Population of Molecules at Microscopic Liquid and Solid Surfaces. *J. Phys. Chem. B* **1998**, *102*, 4446–4450.
- (49) Schlossman, M. L.; Tikhonov, A. M. Molecular Ordering and Phase Behavior of Surfactants at Water-Oil Interfaces as Probed by X-Ray Surface Scattering. *Annu. Rev. Phys. Chem.* **2008**, *59*, 153–177.
- (50) Caminati, G.; Senatra, D.; Gabrielli, G. 1-Hexanol and 1-Tetradecanol Adsorption at the Water Oil Interface. *Langmuir* **1991**, *7*, 1969–1974.
- (51) Scheu, R.; Chen, Y.; de Aguiar, H. B.; Rankin, B. M.; Ben-Amotz, D.; Roke, S. Specific Ion Effects in Amphiphile Hydration and Interface Stabilization. *J. Am. Chem. Soc.* **2014**, *136*, 2040–2047.
- (52) Samson, J. S.; Scheu, R.; Smolentsev, N.; Rick, S. W.; Roke, S. Sum Frequency Spectroscopy of the Hydrophobic Nanodroplet/Water Interface: Absence of Hydroxyl Ion and Dangling OH Bond Signatures. *Chem. Phys. Lett.* **2014**, *615*, 124–131.
- (53) de Beer, A. G. F.; Campen, R. K.; Roke, S. Separating Surface Structure and Surface Charge with Second-Harmonic and Sum-Frequency Scattering. *Phys. Rev. B: Condens. Matter Mater. Phys.* **2010**, *82*, 235431–235431.

(54) Schürer, B.; Wunderlich, S.; Sauerbeck, C.; Peschel, U.; Peukert, W. Probing Colloidal Interfaces by Angle-Resolved Second Harmonic Light Scattering. *Phys. Rev. B: Condens. Matter Mater. Phys.* **2010**, *82*, 241404–241404.

(55) Vácha, R.; Rick, S. W.; Jungwirth, P.; de Beer, A. G. F.; de Aguiar, H. B.; Samson, J. S.; Roke, S. The Orientation and Charge of Water at the Hydrophobic Oil Droplet-Water Interface. *J. Am. Chem. Soc.* **2011**, *133*, 10204–10210.

(56) de Aguiar, H. B.; Scheu, R.; Jena, K. C.; de Beer, A. G. F.; Roke, S. Comparison of Scattering and Reflection SFG: A Question of Phase-Matching. *Phys. Chem. Chem. Phys.* **2012**, *14*, 6826–6832.

(57) de Aguiar, H. B.; Samson, J. S.; Roke, S. Probing Nanoscopic Droplet Interfaces in Aqueous Solution with Vibrational Sum-Frequency Scattering: A Study of the Effects of Path Length, Droplet Density and Pulse Energy. *Chem. Phys. Lett.* **2011**, *512*, 76–80.